Replication fork stalling in WRN-deficient cells is overcome by prompt activation of a MUS81-dependent pathway

Annapaola Franchitto,[1] Livia Maria Pirzio,[1] Ennio Prosperi,[2] Orazio Sapora,[1] Margherita Bignami,[1] and Pietro Pichierri[1]

[1]Section of Experimental and Computational Carcinogenesis, Istituto Superiore di Sanità, 00161 Rome, Italy
[2]Istituto di Genetica Molecolare del Consiglio Nazionale delle Ricerche, sez. Istochimica e Citometria, 27100 Pavia, Italy

Failure to stabilize and properly process stalled replication forks results in chromosome instability, which is a hallmark of cancer cells and several human genetic conditions that are characterized by cancer predisposition. Loss of WRN, a RecQ-like enzyme mutated in the cancer-prone disease Werner syndrome (WS), leads to rapid accumulation of double-strand breaks (DSBs) and proliferating cell nuclear antigen removal from chromatin upon DNA replication arrest. Knockdown of the MUS81 endonuclease in WRN-deficient cells completely prevents the accumulation of DSBs after fork stalling. Also, MUS81 knockdown in WS cells results in reduced chromatin recruitment of recombination enzymes, decreased yield of sister chromatid exchanges, and reduced survival after replication arrest. Thus, we provide novel evidence that WRN is required to avoid accumulation of DSBs and fork collapse after replication perturbation, and that prompt MUS81-dependent generation of DSBs is instrumental for recovery from hydroxyurea-mediated replication arrest under such pathological conditions.

Introduction

Studies from model organisms suggest that stalled replication forks are stabilized by checkpoint proteins and enzymes that contribute to remove the cause of the arrest, for instance secondary DNA structures or protein–DNA complexes, facilitating restart of DNA synthesis once the block is relieved (Branzei and Foiani, 2005). Alterations in the pathway involved in the recovery of stalled forks cause genome instability and chromosomal rearrangements, which are hallmarks of cancer cells and chromosome fragility syndromes (Myung et al., 2001; Taylor, 2001). Thus, unveiling the mechanisms of replication fork recovery in human cells is of paramount importance. However, little is known about the mechanisms of fork recovery both under physiological and pathological conditions in human cells. In this regard, cell lines from patients bearing mutations in replication-related caretaker genes may be of utmost importance as a model to investigate how recovery of stalled forks is performed and regulated in humans.

Werner syndrome (WS) is a rare hereditary disease featuring premature aging and enhanced cancer predisposition (Chen and Oshima, 2002). WS cells are characterized by reduced replicative potential, S-phase defects, chromosome rearrangements, and hypersensitivity to replication-perturbing agents, all of which are phenotypes directly related to defective handling of stalled forks (Franchitto and Pichierri, 2002). The protein mutated in WS, WRN, belongs to the RecQ class of DNA helicases, a family of enzymes that have been largely implicated in the response to perturbed replication. However, how WRN contributes to the safe handling of stalled forks and whether the WS cellular phenotype derives from harmful attempts of DNA synthesis recovery is still debated.

Consistent with in vitro substrate preference, WRN has been proposed to reset reversed forks or other replication intermediates arising after fork stalling, clearing the way to replisome progression once the block is removed (Khakhar et al., 2003). Alternatively, WRN has been implicated in the resolution of recombination intermediates arising after RAD51-dependent strand invasion (Saintigny et al., 2002).

Correspondence to Pietro Pichierri: pietro.pichierri@iss.it

Abbreviations used in this paper: ATR, ataxia telangiectasia and Rad3–related; CENP-F, centromere protein F; CldU, chlorodeoxyuridine; DSB, double-strand break; HJ, Holliday junction; HU, hydroxyurea; IdU, iododeoxyuridine; PCNA, proliferating cell nuclear antigen; PFGE, pulsed-field gel electrophoresis; SCE, sister chromatid exchange; WS, Werner syndrome.

The online version of this paper contains supplemental material.

The Rockefeller University Press $30.00
J. Cell Biol. Vol. 183 No. 2 241–252
www.jcb.org/cgi/doi/10.1083/jcb.200803173

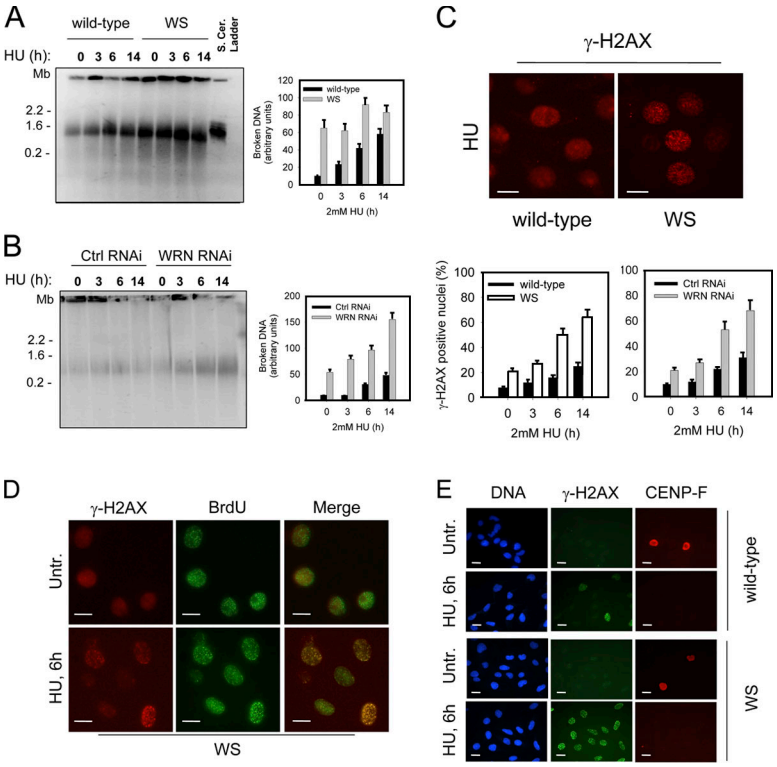

Figure 1. **WRN deficiency leads to accumulation of DSBs in S phase after replication fork arrest.** (A) Formation of DSBs in wild-type and WS fibroblasts was evaluated by PFGE after 3-, 6-, and 14-h 2 mM HU treatment. The graph shows quantification of DSBs from three independent experiments. Data are presented as mean ± SE. (B) Formation of DSBs in HeLa cells transfected with control (GFP) or WRN siRNAs was evaluated by PFGE after exposure to 2 mM HU for 3, 6, and 14 h. The graph shows quantification of DSBs from three independent experiments. Data are presented as mean ± SE. (C) Analysis of DSB accumulation by anti–γ-H2AX immunofluorescence. Wild-type, WS, and HeLa cells transfected with control (GFP) or WRN siRNAs were treated with 2 mM HU for the indicated times. Images show wild-type and WS cells treated with 2 mM HU for 6 h. Graphs show the percentage of γ-H2AX–positive nuclei in wild-type, WS (left), or HeLa cells transfected with control (GFP) or WRN siRNAs (right). Data are presented as mean ± SE from three independent experiments. (D) Colocalization of DSBs and replicating DNA. Wild-type and WS fibroblasts were labeled with BrdU for 30 min before addition of 2 mM HU for 6 h. Replicating DNA was visualized using anti-BrdU antibodies, whereas DSBs were labeled with anti–γ-H2AX. (E) Double immunostaining with the G2-phase marker CENP-F and anti–γ-H2AX antibodies. Wild-type and WS cells were treated with 2 mM HU for 6 h. Bars, 10 μM.

Cells mutated in WRN accumulate DNA breaks if challenged with replication-perturbing agents, which is indicative of incorrect handling of stalled forks (Pichierri et al., 2001). However, WS cells are able to recover from DNA synthesis perturbation, which suggests that loss of WRN is compensated by alternative pathways.

MUS81 is a specialized endonuclease that forms a heterodimer with EME1 and processes Holliday junctions (HJs) and other branched replication or recombination intermediates (Haber and Heyer, 2001; Osman and Whitby, 2007). Recently, MUS81 has been involved in the stabilization of chromatin-bound proliferating cell nuclear antigen (PCNA) and in the cellular recovery upon replication arrest in human cells (Hanada et al., 2007; Shimura et al., 2008). In yeasts, mutations of the RecQ helicase Sgs1 or Rqh1 are synthetic lethal with mutations in MUS81 (Boddy et al., 2000; Kaliraman et al., 2001; Mullen et al., 2001). The observation that mutation in MUS81 reduces viability of RecQ-defective yeasts after fork stalling suggested that these two proteins may function on common substrates in response to replication stress, defining two parallel branches of the replication fork recovery pathway.

Here, we investigated whether WRN deficiency might be backed up by MUS81-dependent processing of replication intermediates formed at stalled forks.

We provide evidence that loss of WRN results in fork collapse and that double-strand breaks (DSBs) accumulating in WRN-deficient cells derive from MUS81-dependent processing. We further demonstrate that, in the absence of WRN, MUS81 is required for the accumulation in chromatin of both RAD51 and RAD52 and for replication recovery. Indeed, depletion of MUS81 by RNAi in WRN-deficient backgrounds significantly impairs survival after hydroxyurea (HU) arrest, which suggests that the MUS81 branch is necessary to ensure cellular viability in WS, perhaps at the expense of genomic stability.

Results

WRN prevents accumulation of DSBs during DNA synthesis upon replication fork stalling

Mutations in vertebrate and mammalian genes associated with the replication stress response, such as ataxia telangiectasia and Rad3–related (ATR), determine the appearance of DNA breaks in replicating cells (Cliby et al., 1998; Casper et al., 2002; Lomonosov et al., 2003; Trenz et al., 2006). Thus, to investigate whether loss of WRN could influence DSB formation during DNA replication, we inhibited DNA synthesis in wild-type and WS cells with HU. We evaluated DSB induction in the whole genome using pulsed-field gel electrophoresis (PFGE) and, at the single-cell level, anti–phospho-H2AX (γ-H2AX) immunostaining. Formation of chromosomal breaks was analyzed early after HU-mediated replication arrest and up to 14 h, a timepoint corresponding to accumulation of DSBs in the wild type (Saintigny et al., 2001). WRN deficiency resulted in enhanced accumulation of DSBs under unstressed conditions and at early time points after HU treatment. In contrast, wild-type cells accumulated DSBs only at the 14 h time point (Fig. 1 A). To confirm correlation between loss of WRN function and accumulation of DSBs after replication arrest in a common genetic background, we transfected WRN siRNAs in HeLa cells and then analyzed DSB formation after HU by PFGE. RNAi efficiently depleted WRN protein from HeLa cells (see Fig. 3 B), conferring

a WS-like phenotype of hypersensitivity to camptothecin (unpublished data). Down-regulation of WRN by RNAi determined a time-dependent increase in the accumulation of DSBs in response to HU treatment, whereas chromosomal fragmentation was barely detectable after transfection with control siRNAs (Fig. 1 B). Morphological inspection of HU-treated cultures did not provide evidence of cell death, which excludes the possibility that chromosomal fragmentation derived from the induction of apoptosis (unpublished data).

Formation of γ-H2AX foci is widely used as a marker of DSBs and is also thought to correlate with replication-associated DSBs (Ward and Chen, 2001). Thus, we performed γ-H2AX immunostaining in WRN-deficient cells as an independent approach to evaluate formation of DSBs after HU treatment. Although a limited time-dependent increase of γ-H2AX–positive nuclei was observed in wild-type cells after replication arrest, a marked enhancement of γ-H2AX foci was detected in WS fibroblasts after HU treatment (Fig. 1 C). Similarly, WRN RNAi, but not transfection with control siRNAs, determined a consistent increase in γ-H2AX–positive nuclei, either in response to HU or simply under unperturbed cell growth (Fig. 1 C). To further confirm our findings, accumulation of DSBs was also analyzed in WS lymphoblasts and their WRN-complemented counterparts. Both PFGE and γ-H2AX immunostaining revealed a marked increase of DSBs depending on the WRN status of the cells (Fig. S1, available at http://www.jcb.org/cgi/content/full/jcb.200803173/DC1).

To verify whether DSBs were actually taking place in replicating cells, we labeled S-phase wild-type and WS fibroblasts with a short pulse of BrdU before adding HU for 6 h. The occurrence of DSBs in replicating cells was evaluated by simultaneous BrdU/γ-H2AX immunostaining. The totality of γ-H2AX–positive nuclei was BrdU positive in unstressed and HU-treated WS cells (Fig. 1 D). To exclude the possibility that DSBs could arise in G2 phase, parallel samples were stained with anti–centromere protein F (CENP-F) antibodies, which are an acknowledged G2 marker (Rattner et al., 1993). Combined γ-H2AX and CENP-F immunofluorescence showed that γ-H2AX–positive nuclei were always CENP-F negative (Fig. 1 E). Accumulation of DSB in WS cells after HU treatment was not paralleled by a defect in the activation of the ATR-dependent checkpoint, as shown by comparable levels of S345-phosphorylated CHK1 between control and WRN RNAi-treated cells (Fig. S2, available at http://www.jcb.org/cgi/content/full/jcb.200803173/DC1).

Altogether, our data show that loss of WRN determines an enhanced accumulation of DSBs in S-phase cells after replication inhibition by HU.

The MUS81 endonuclease is required to induce DSBs in WRN-deficient cells after replication fork stalling

Having demonstrated that WS cells accumulate DSBs after HU-induced replication arrest, we asked whether those DSBs could be the end result of the action of a backup pathway processing replication intermediates in the absence of WRN. In yeast, mutations in the RecQ helicases, Sgs1 or Rqh1, are synthetic lethal, with a mutation inactivating the Mus81–Eme1 complex, which indicates that RecQ helicases and the Mus81 endonuclease can define two competing pathways processing branched DNA intermediates at stalled replisome (Boddy et al., 2001; Doe et al., 2002; Ciccia et al., 2003; Whitby et al., 2003; Cotta-Ramusino et al., 2005; Fricke et al., 2005). Furthermore, a recent paper suggests that the MUS81 function could be required to process forks stalled at interstrand DNA crosslink sites forming DSBs (Hanada et al., 2006). We investigated whether the genetic interaction observed in yeast was conserved in humans by testing the hypothesis that MUS81 could be involved in DSB formation in a WRN-deficient background. To this end, we used siRNA-mediated RNAi to down-regulate MUS81 expression in either WS or HeLa cells. Under our experimental conditions, RNAi reduced MUS81 expression of >80% in wild-type, WS, and HeLa cells (Fig. 2, A and B), and did not alter cell cycle progression (Fig. S3, A and B, available at http://www.jcb.org/cgi/content/full/jcb.200803173/DC1). 48 h after transfection, replication fork arrest was induced with HU, and DSBs were evaluated by PFGE. In wild-type fibroblasts or HeLa cells, MUS81 RNAi did not significantly affect DSB formation after HU treatment, at least up to 14 h of replication arrest (Fig. 2, C and D). In contrast, depletion of MUS81 in WRN-deficient fibroblasts or concomitant knockdown of WRN and MUS81 in HeLa cells decreased the amount of DSBs induced by replication fork stalling close to that observed in untreated controls (Fig. 2, C and D). Notably, MUS81 down regulation also reduced the spontaneous level of DNA breaks observed in WRN-deficient cells (Fig. 2 C), even though it failed to modulate the breakage in untreated WRN RNAi HeLa cells (Fig. 2 D). This apparent discrepancy could depend on the enhanced level of MUS81-related DSBs accumulating as a consequence of chronic versus acute WRN depletion and the PFGE threshold of detection, could be related to a more efficient MUS81 silencing in WS cells, or could be combination of both. However, analysis of the induction of γ-H2AX foci in HeLa cells treated with WRN or WRN/MUS81 siRNAs revealed a drastic reduction of γ-H2AX immunostaining in HU-treated cells and untreated samples as well (Fig. 2 E). A consistent reduction of DSBs evaluated by γ-H2AX immunofluorescence was found also in HU-treated WS cells upon transfection with MUS81 siRNAs (unpublished data). It is worthwhile to note that accumulation of DSBs after treatment with the topoisomerase II–poison etoposide was independent of the presence of WRN and MUS81 (Fig. 2 C), which suggests that MUS81 cleavage is not involved in DSB formation when DSBs are formed directly, as occurs after inhibition of topoisomerase II by etoposide.

In fission yeast, activation of MUS81 results in its chromatin accumulation (Kai et al., 2005); thus, we investigated whether WRN-deficient cells presented enhanced chromatin binding of MUS81 after replication fork arrest. To this end, control and WRN RNAi-treated HeLa cells were exposed to HU and analyzed for the presence of chromatin-bound MUS81 at different time points through biochemical fractionation and immunoblotting.

In control HeLa cells, the fraction of chromatin-associated MUS81 is low and barely increased after replication arrest, whereas the amount of chromatin-bound MUS81 was enhanced

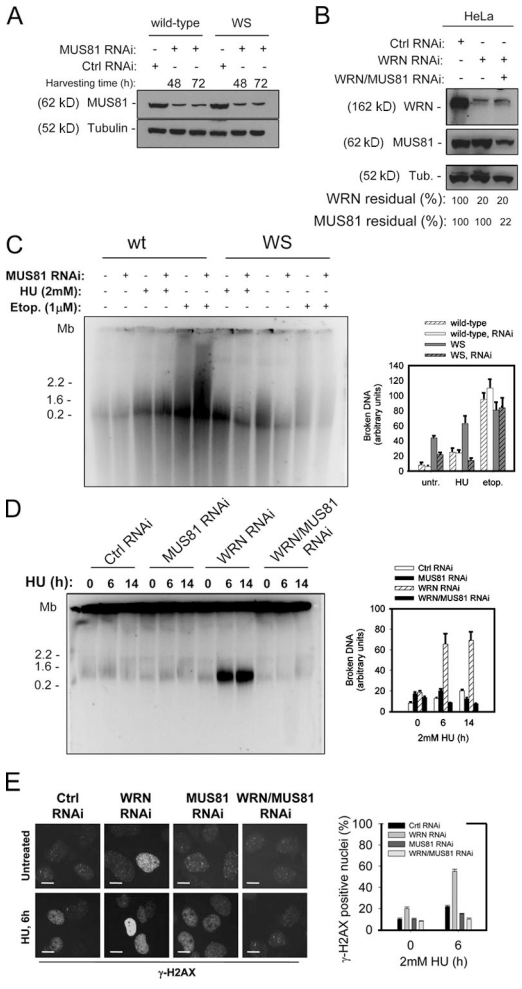

Figure 2. **Accumulation of DSBs after replication arrest observed in the absence of WRN depends on the presence of the MUS81 endonuclease.** (A) MUS81 down-regulation by transfection of MUS81 siRNAs in wild-type and WS cells. (B) MUS81 and/or WRN down-regulation by transfection of MUS81 and/or WRN siRNAs in HeLa cells was verified by immunoblotting 48 h after transfection. (C) Formation of DSBs in wild-type and WS fibroblasts transfected with MUS81 siRNAs was evaluated by PFGE after 6 h of treatment with 2 mM HU or 1 μM etoposide (Etop.). Data are presented as mean ± SE from three independent experiments. (D) Formation of DSBs in HeLa cells transfected with control (GFP), MUS81, and/or WRN siRNAs and treated with 2 mM HU for the indicated times was evaluated by PFGE. Data are presented as mean ± SE from three independent experiments. (E) Analysis of DSB accumulation by anti–γ-H2AX immunofluorescence in HeLa cells transfected with control (GFP), MUS81, and/or WRN siRNAs and treated with 2 mM HU for 6 h. Representative images are shown. The percentage of γ-H2AX–positive nuclei from three independent experiments is shown. Data are presented as mean ± SE. Bars, 10 μM.

in WRN RNAi-treated cells under unperturbed conditions and increased by >50% readily after HU treatment, maintaining sustained levels at later times as well (Fig. 3). Because the fraction of S- and G2-phase cells was not different between control and WRN RNAi cells (Fig. S4, available at http://www.jcb.org/cgi/content/full/jcb.200803173/DC1; and not depicted), it is unlikely that the observed increased chromatin binding of MUS81 in WRN-depleted cells can be ascribed to a difference in cell cycle progression.

Altogether, the results of the PFGE analyses and the γ-H2AX immunostaining indicate that MUS81 is required to form

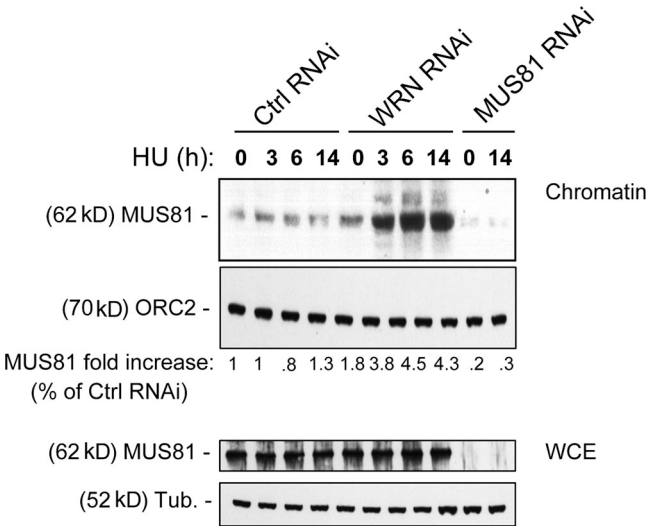

Figure 3. **Loss of WRN results in enhanced association of MUS81 with chromatin after replication fork stalling.** Levels of chromatin-bound and total MUS81 in HeLa cells transfected with control (GFP), WRN, or MUS81 siRNAs and treated with 2 mM HU for indicated times. ORC2 was used as a loading control. The amount of MUS81 in the chromatin fraction is expressed as the percentage of the amount in the untreated control normalized against the ORC2 content. (bottom) Total content of MUS81 in RNAi-treated HeLa cells was evaluated by Western immunoblotting after treatment with 2 mM HU, as in Fig. 2.

DSBs after replication fork stalling in the absence of WRN protein. Moreover, the enhanced chromatin association of MUS81 observed in WRN-deficient cells reinforces the hypothesis that MUS81 is acting to process replication intermediates, which are otherwise targeted by WRN.

Dissociation of PCNA from S-phase chromatin after replication fork stalling occurs in the absence of WRN and is not prevented by MUS81 down-regulation

Formation of DSBs after replication fork stalling often correlates with replication fork collapse, i.e., replisome dissociation from the stalled fork (Branzei and Foiani, 2005), a phenomenon that can be visualized by monitoring either dissociation of replicative polymerases, especially Polε, or dispersal of the so-called replication factories (Montecucco et al., 2001; Cobb et al., 2003; Lucca et al., 2004). Dispersal of replication factories has been visualized at the single-cell level using PCNA immunostaining after extraction of the entire non-chromatin-associated fraction. To investigate whether, in WS cells, DSB accumulation after HU treatment was correlated to fork collapse, we analyzed chromatin association of PCNA by Western blotting or biparametric flow cytometry (Scovassi and Prosperi, 2006).

To validate our approach, we treated cells with 50 μM etoposide, a condition found to determine >80% of replisome disassembly as visualized at the single-cell level by PCNA staining (Montecucco et al., 2001). Our assays proved to be able to detect etoposide-induced replisome disassembly, and, thus, we consider it equivalent to the in situ assay used by Montecucco et al., (2001) and useful to investigate replisome collapse after HU treatment. Analysis of chromatin fractions revealed that

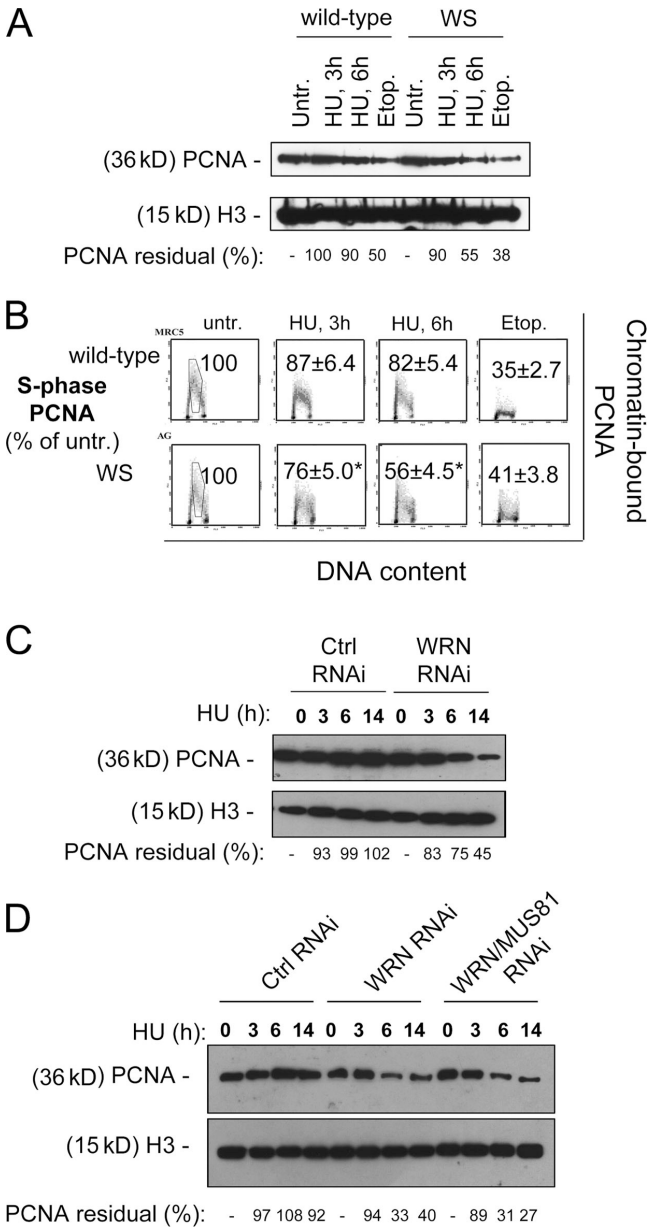

Figure 4. **Replication arrest induces dispersal of PCNA from S-phase chromatin in WRN-deficient cells.** (A) Levels of chromatin-bound PCNA in wild-type and WS fibroblasts treated with 2 mM HU for the indicated times or with 50 µM etoposide for 6 h (Etop.). H3 histone was used as a loading control. The residual amount of PCNA in the chromatin fraction is expressed as the percentage of the amount in the untreated control normalized against the H3 histone content. (B) Levels of chromatin-bound PCNA in S-phase cells after replication inhibition. Wild-type and WS fibroblasts were exposed to 2 mM HU for the indicated times or to 50 µM etoposide for 6 h (Etop.), before being processed for biparametric PCNA/DNA flow cytometry. Representative cytograms for each condition are presented. The values shown represent the fluorescence intensity of the PCNA staining relative to an S-phase DNA content, expressed as percentage of the untreated control. The gates indicate the area considered for the evaluation of PCNA fluorescence intensity. *, statistically significant compared with the wild type; $P < 0.01$ (analysis of variance test). (C) Levels of chromatin-bound PCNA in HeLa cells transfected with control (GFP) or WRN siRNAs and treated with 2 mM HU for the indicated times. H3 histone was used as a loading control. The residual amount of PCNA in the chromatin fraction is expressed as the percentage of the amount in the untreated control normalized against the H3 histone content. (D) Levels of chromatin-bound PCNA in HeLa cells transfected with control (GFP), MUS81, and/or WRN siRNAs treated with 2 mM HU for the indicated times. H3 histone was determined as a loading control. RNAi-labeled samples represent cells treated with MUS81 siRNAs; if not otherwise specified, samples were treated with control siRNAs against GFP.

HU-induced replication fork stalling did not induce an overt dissociation of PCNA from chromatin in wild-type cells, whereas WRN deficiency determined a much more substantial decrease (Fig. 4 A). In contrast, etoposide treatment, which directly causes DSBs irrespective of the WRN status of the cells, dropped the amount of chromatin-associated PCNA in both wild-type and WS cells (Fig. 4 A). Flow cytometry analysis confirmed that a significant fraction of PCNA dissociates from chromatin in WS cells treated with HU, and evidenced that loss of PCNA occurred specifically in S-phase cells (Fig. 4 B).

The requirement of WRN in preventing dissociation of PCNA from S-phase chromatin after HU-mediated replication fork stalling was also confirmed by using RNAi to knock down WRN functions in HeLa cells before inducing replication stress. As shown in Fig. 4 C, WRN RNAi, but not transfection with control siRNAs, reduced the amount of PCNA associated with chromatin after HU treatment. Having demonstrated that in WS cells a MUS81-dependent mechanism produced DSBs after replication fork stalling, we asked whether chromatin dissociation of PCNA was dependent on MUS81. Thus, HeLa cells were transfected with WRN siRNAs alone or in combination with MUS81 siRNAs, then exposed to HU and fractionated to analyze subcellular distribution of PCNA by Western blotting. Fig. 4 D shows that PCNA dissociated from chromatin irrespective of the presence of MUS81 in WRN-depleted cells.

To further demonstrate occurrence of replication fork collapse in WRN-deficient cells after treatment with HU, we measured the efficiency of replication recovery using the DNA fiber assay (Merrick et al., 2004; Seiler et al., 2007). To this end, DNA replication sites were pulse-labeled using chlorodeoxyuridine (CldU) before HU treatment. After replication fork stalling, cells were washed and pulse-labeled with iododeoxyuridine (IdU) to visualize the restart of stalled forks (Fig. S5 A, available at http://www.jcb.org/cgi/content/full/jcb.200803173/DC1). CldU-labeled, red tracks represent stalled forks that did not recover DNA replication (i.e., collapsed forks), whereas red tracks showing costaining with green IdU-labeled tracks represent stalled forks that restore properly DNA replication (Fig. S5, A and B). In control RNAi-treated cells, almost all the stalled forks recovered upon HU withdrawal, whereas only half of the ongoing forks restarted in WRN RNAi cells (Fig. S5 C). It is worthwhile to note that our data on the collapse of stalled forks by the DNA fiber assay are in good agreement with PCNA dissociation from chromatin, obtained by either biochemical fractionation or flow cytometry. The DNA fiber assay also confirmed that fork collapse occurs independently of MUS81 because the number of restarting forks was not affected by concomitant depletion of WRN and MUS81 (Fig. S5 D).

These results indicate that in WS cells, MUS81-dependent DSB accumulation takes place after fork collapse.

It has been previously demonstrated that dispersal of replication foci after etoposide-induced replication fork collapse relies on the ATR-dependent checkpoint (Rossi et al., 2006).

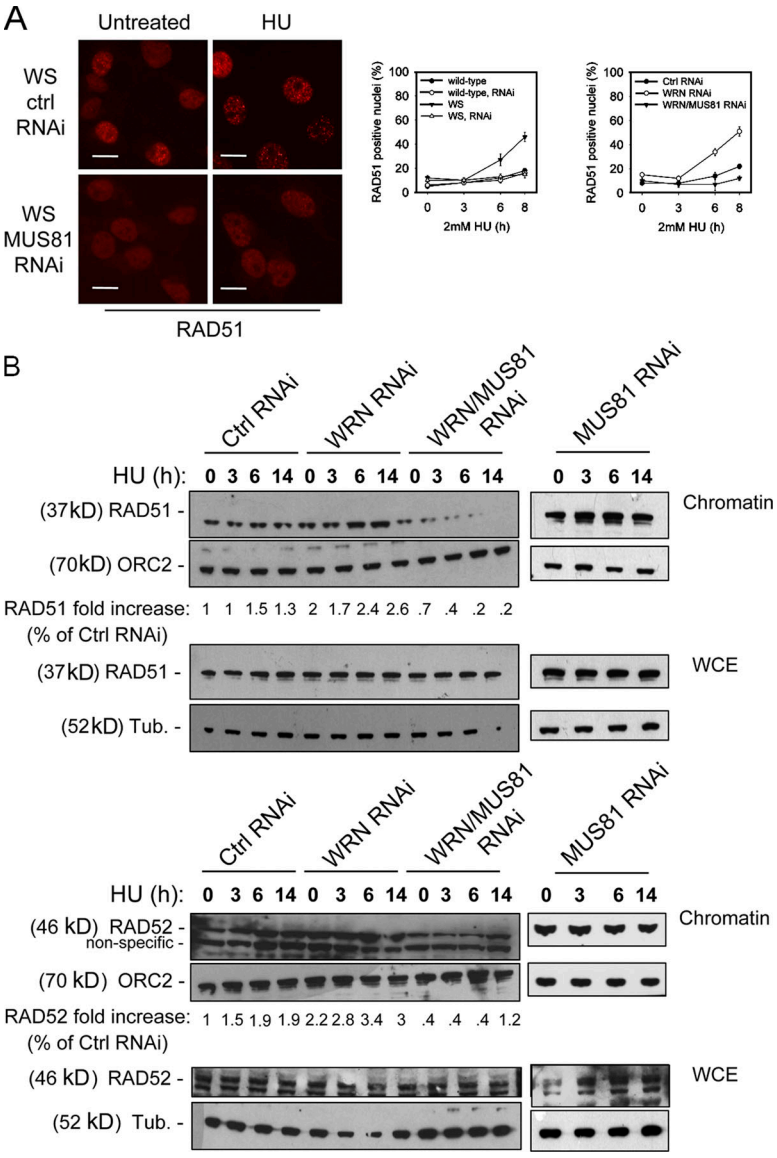

Figure 5. **MUS81 down-regulation reduces the assembly in nuclear foci and chromatin binding of RAD51 in WS cells after replication arrest.** (A) RAD51 assembly in nuclear foci after HU treatment. Wild-type and WS fibroblasts were transfected with control or MUS81 siRNAs and exposed to 2 mM HU for the indicated times. Representative images of RAD51 assembly in nuclear foci induced by MUS81 RNAi in WS cells treated with 2 mM HU for 8 h were shown. The graph shows the percentage of RAD51-positive nuclei in wild-type and WS cells transfected with control (GFP) or MUS81 siRNAs (left graph), or Hela cells transfected with control (GFP), WRN, or WRN/MUS81 siRNAs (right graph). Data are means ± SE from three independent experiments. Bars, 10 µM. (B) Levels of chromatin-bound and total RAD51 or RAD52 in HeLa cells transfected with control (GFP), WRN, and WRN/MUS81 siRNAs and treated with 2 mM HU (HU) for the indicated times. The amount of RAD51 and RAD52 in the chromatin fraction was presented as fold increase compared with the matched untreated control, normalized against the amount of ORC2. The levels of chromatin-associated and total RAD51/RAD52 proteins observed in MUS81-depleted cells are shown as a control.

Thus, we analyzed whether dissociation of PCNA from chromatin in the absence of WRN was related to the ATR-dependent checkpoint. To this end, we down-regulated ATR expression by RNAi (Fig. S5 A) and examined PCNA chromatin association in fractionated extracts from untreated or HU-exposed cells. We observed that PCNA dissociation from chromatin was ATR dependent after etoposide treatment, irrespective of the presence of WRN (Fig. S5 B). Likewise, loss of PCNA from chromatin observed in the absence of WRN after HU treatment was reverted by depletion of ATR by RNAi (Fig. S5 B).

Altogether, these results show that loss of WRN determines collapse of stalled forks in a MUS81-independent but ATR-dependent manner.

MUS81 is required for replication arrest–dependent recombination observed in the absence of WRN

The DNA DSBs formed by MUS81 at stalled forks in WRN-deficient cells could be easily used as substrate to initiate recombination-mediated fork recovery. Indeed, a physical interaction between MUS81 and recombination enzymes has been described in yeast and mammalian cells (Interthal and Heyer, 2000; Hanada et al., 2006). To investigate whether DSBs produced by MUS81 could initiate recombination at forks collapsed because of loss of WRN function, we analyzed the accumulation of RAD51 in nuclear foci and its chromatin binding in cells depleted of WRN, MUS81, or both by RNAi. Chromatin association of the recombination mediator protein RAD52 was similarly analyzed. Induction of replication arrest with HU induced RAD51 accumulation in nuclear foci in a time-dependent manner, and the RAD51 focus-forming activity appeared enhanced in WS cells compared with the wild type (Fig. 5 A), which is in agreement with our previous studies (Pichierri et al., 2001). Consistent findings were observed in HeLa cells upon depletion of WRN by RNAi (Fig. 5 A), which demonstrates that increased RAD51 assembly into nuclear foci directly correlates with the absence of WRN. Depletion of MUS81 in WS fibroblasts or concomitant knockdown of WRN and MUS81 in HeLa cells

strongly reduced the number of RAD51 foci observed after replication stalling (Fig. 5 A). Consistent findings were observed by biochemical fractionation analysis. Chromatin binding of RAD51 was enhanced in WRN RNAi HeLa cells after HU treatment and was extremely reduced upon concomitant depletion of MUS81 (Fig. 5 B). Chromatin binding of the recombination-mediator protein RAD52 was also enhanced by loss of WRN, and when MUS81 was down-regulated, a clear reduction in the amount of protein that associates with chromatin was observed (Fig. 5 B). Interestingly, both RAD51 and RAD52 were found to be more chromatin-associated in WRN-depleted cells even under unperturbed conditions, and such enhanced chromatin association was reduced after MUS81 knockdown (Fig. 5 B). In contrast, the MUS81 down-regulation simply did not reduce RAD51 and RAD52 chromatin binding in control HeLa cells or wild-type cells (Fig. 5 B and not depicted).

The immunofluorescence and biochemical fractionation experiments indicated that DSBs produced by MUS81 stimulate assembly of recombination foci and chromatin association of recombination proteins after replication stalling, which suggests that in the absence of WRN, MUS81 can be recruited upstream of recombination. To support our hypothesis, we analyzed whether the enhanced MUS81 chromatin association observed in the absence of WRN was affected by down-regulation of the RAD51 protein. We reasoned that if MUS81 actually acts before recombination, its association with chromatin should be independent from strand invasion. We efficiently depleted RAD51 in HeLa cells, with or without concomitant depletion of WRN (Fig. S5 C), and found that MUS81 association with chromatin was still enhanced by loss of WRN after RAD51 knockdown (Fig. S5 D). Then we evaluated the yield of HU-induced sister chromatid exchanges (SCEs) in HeLa cells transfected with WRN siRNAs alone or in combination with MUS81 siRNAs. Indeed, DSBs formed at stalled forks are thought to be good SCE inducers (Arnaudeau et al., 2001; Lambert and Lopez, 2001). Knockdown of WRN alone increased the yield of HU-induced SCEs about threefold compared with the cells transfected with control siRNAs, whereas concomitant depletion of WRN and MUS81 reduced the level of SCEs back to that observed in untreated cultures (Fig. 6). In contrast, no differential induction of SCEs was found after etoposide treatment between control and WRN RNAi-treated cells, and no modulation by MUS81 was observed (Fig. 6).

These findings show that loss of WRN promotes the accumulation of recombination factors in chromatin and stimulates SCEs after HU-mediated replication arrest. Moreover, they evidenced that increased chromatin binding of recombination proteins and elevated recombination are prevented by MUS81 knockdown, which suggests that MUS81-dependent DSBs created at stalled forks are used as a substrate to initiate recombination.

In WS cells, MUS81 is required to ensure recovery from replication arrest and cellular viability

In response to HU-mediated replication fork stalling, WRN-deficient cells require MUS81 to produce DSBs and initiate recombination. These data are consistent with the notion that WRN and MUS81 operate in two parallel branches of the response to replication stress, which suggests that MUS81 down-regulation could affect recovery of WRN-deficient cells from the HU-mediated replication arrest.

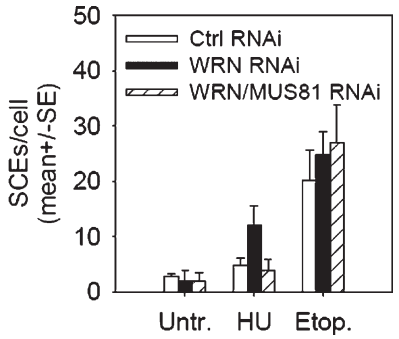

Figure 6. **MUS81 depletion affects the recombination-mediated repair of stalled forks.** Levels of SCEs induced by HU in HeLa cells transfected with control (GFP), WRN, or WRN/MUS81 siRNAs and treated for 16 h with 2 mM HU (HU) or 300 nM etoposide (Etop.). Error bars represent SEM.

To test this hypothesis, WS fibroblasts and HeLa cells RNA depleted of WRN alone or in combination with MUS81 were exposed to HU for 16 h, then recovered in drug-free medium for different times. 30 min before harvesting, cells were pulsed with BrdU to evaluate DNA synthesis. Alternatively, wild-type and WS fibroblasts were transfected with MUS81 siRNAs and analyzed for the presence of chromosomal damage after recovery from HU. Loss of WRN function alone did not influence arrest and recovery of DNA synthesis after HU (Figs. S3 and S4). In contrast, concomitant MUS81 inhibition by RNAi in WS fibroblasts or in HeLa cells knocked down for WRN significantly impaired the ability of HU-arrested cells to resume DNA synthesis (Fig. 7 A). Furthermore, MUS81 RNAi in WS cells that are recovered from HU-mediated S-phase arrest resulted in the appearance of aberrant metaphases with fuzzy chromosomes and in micronuclei (Fig. 7 B and not depicted).

To further demonstrate that MUS81 is required for efficient recovery from replication arrest in a WRN-deficient background, we abrogated the WRN function alone or in combination with MUS81, exposed cells to 14 h of different doses of HU, and compared the clonogenic survival 7 d thereafter. As shown in Fig. 7 C, concomitant down-regulation of WRN and MUS81 determined a striking reduction in survival after 14 h of HU-mediated replication arrest compared with control RNAi and WRN RNAi cells.

Altogether, these results show that in WS cells, efficient recovery from DNA replication arrest and maintenance of cellular viability depends on the activation of an alternative pathway of replication fork processing requiring the MUS81 protein.

Discussion

Here, we demonstrate that in the absence of WRN, cells accumulate DSBs upon replication arrest as a consequence of fork collapse and activation of a MUS81-dependent pathway. Thus, in WRN-deficient cells, the MUS81 endonuclease might represent an alternative pathway to ensure recovery of DNA synthesis by recombination-mediated restart of DNA replication.

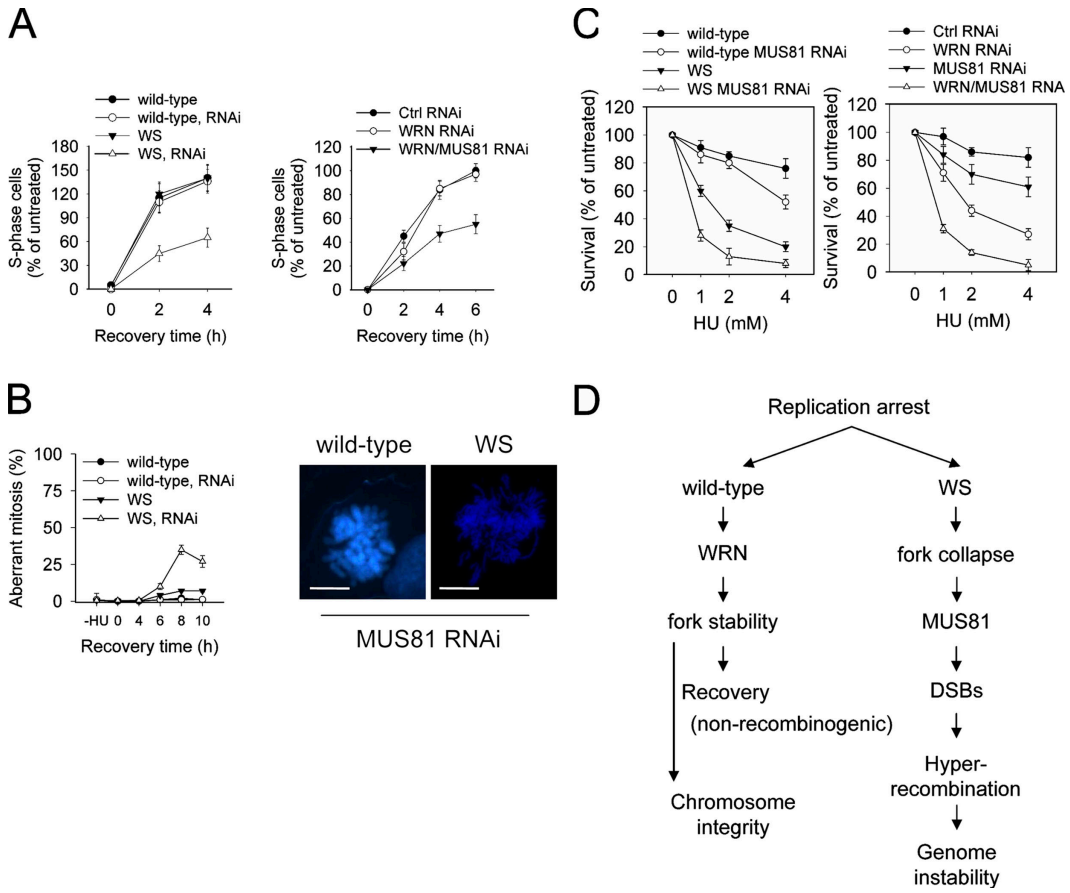

Figure 7. **MUS81 down-regulation reduces the recovery of WS cells from replication arrest, leading to the accumulation of chromosome damage.** (A) Analysis of the inhibition of DNA synthesis in wild-type and WS cells. Wild-type and WS cells transfected with control (GFP) or MUS81 siRNAs (left) and Hela cells transfected with control (GFP), WRN, or WRN/MUS81 siRNAs (right) were treated with 2 mM HU for 14 h, and recovered in drug-free medium for the indicated times. The graphs show the percentage of BrdU-positive nuclei compared with the untreated control. Data are means ± SE from three independent experiments. (B) Analysis of aberrant mitoses induced by replication arrest. Wild-type and WS cells transfected with control (GFP) or MUS81 siRNAs were exposed to 2 mM HU for 18 h before being recovered in drug-free medium for the indicated times. Images show mitoses from wild-type and WS cells in which MUS81 was abrogated. Bars, 20 μM. (C) Survival of wild-type, WS, or HeLa cells transfected with the indicated siRNAs in response to increasing doses of HU. Data are means ± SE from three independent experiments. (D) Schematic model showing the pathways responsible for replication fork recovery in wild-type and WS cells.

In yeast, the RecQ helicase and MUS81/EME1 are synthetic lethal, and lethality is rescued by introduction of a bacterial resolvase, which suggests that these two proteins act in overlapping pathways on a common branched intermediate arising at stalled forks, such as an HJ or a regressed fork (Boddy et al., 2000; Mullen et al., 2001; Doe et al., 2002). Our findings suggest that such genetic interaction is also maintained in humans, and that WRN and MUS81 define two pathways competing for a common substrate at stalled forks, as suggested by their mutually independent subnuclear localization (Gao et al., 2003). WRN helicase activity displays remarkable substrate preference toward forked DNA and several replication intermediates that can accumulate at stalled forks, such as D-loops and four-way junctions (regressed fork; Khakhar et al., 2003), and several of the preferred DNA substrates of WRN are also efficiently processed by human MUS81 (Blais et al., 2004). Indeed, our data support the hypothesis that the two enzymes share common substrates and suggest that WRN could disrupt abnormal replication intermediates, preventing them from being processed by MUS81 and facilitating a safer restart of DNA synthesis. Synthetic lethality of the yeast recq/mus81 double mutant can be prevented by mutations in recombination genes, leading to a model whereby the common substrate of RecQ helicases and MUS81 is formed during recombination-mediated replication fork recovery triggered by single-strand gaps (Fabre et al., 2002). In contrast, we find that, in the absence of WRN, recombination induced by HU treatment is triggered after MUS81 processing of stalled forks, implying that, at least in the absence of WRN, MUS81 functions upstream of recombination. Thus, our data indicate a different behavior of RecQ mutant yeasts and human cells mutated in *WRN*. This is not surprising because humans have five RecQ-like helicases (Hickson, 2003), and many studies evidenced that the functional homologue of yeast RecQ helicase is BLM and not WRN (Yamagata et al., 1998; Ira et al., 2003; Wu and Hickson, 2003). However, at this stage, we cannot exclude the possibility that recombination proteins other than RAD51 and RAD52 might function at stalled forks to produce an intermediate that is then converted into a DSB, which, in turn, recruits RAD52/RAD51 and initiates recombination. Most likely, it is conceivable that

WRN might perform an antirecombinogenic or a prorecombinogenic function according to the nature of the lesion. Upon treatment with agents that directly introduce DSBs or collapse the replication fork, WRN would be required to resolve HJs derived from RAD51-dependent strand invasion (Saintigny et al., 2002). However, our data suggest that, upon replication stalling, WRN would act as an antirecombinogenic enzyme. Indeed, loss of WRN increased both recruitment of recombination proteins and the yield of SCEs after HU treatment. Moreover, abrogation of RAD51-dependent recombination does not revert sensitivity to HU of WS cells, but rather further reduces viability of WRN-deficient cells upon replication stress (unpublished data).

We show that loss of WRN determines unloading of PCNA from replicative chromatin after HU treatment, which indicates that blocked forks may collapse in WS cells. It has been recently found that in *Schizosaccharomyces pombe*, recruitment of MUS81 to chromatin after replication fork stalling is inhibited, whereas its association with chromatin is strongly stimulated by fork collapse (Kai et al., 2005). We also show that human MUS81 does not normally accumulate in chromatin upon fork stalling, at least within 14 h of arrest. In contrast, MUS81 is rapidly recruited to chromatin in the absence of WRN, which is consistent with the collapse of stalled forks. These results support the idea that the MUS81-dependent pathway is not promptly activated in human cells by replication arrest after an acute exposure to HU, possibly to avoid formation of dangerous DSBs at stalled forks. Accordingly, MUS81-deficient cells are not hypersensitive to acute HU treatment, although they show heightened sensitivity toward agents inducing fork collapse, such as cisplatin or mitomycin-C (McPherson et al., 2004; Dendouga et al., 2005; Hanada et al., 2006), These data suggest that the caretaker function of MUS81 is linked to repair of spontaneously collapsed rather than blocked replication forks. Interestingly, although a recent paper from Hanada et al., (2007) confirms our observations that MUS81 is not activated after short exposure to HU, the same work demonstrates that prolonged treatment with HU (18–24 h) results in the formation of MUS81-dependent DSBs. Those DSBs result from the processing of RAD51-dependent intermediates, and, thus, would represent a different mechanism from that disclosed by our data. Probably, in wild-type cells, recombination initiated from stalled forks cannot be terminated properly when replication is still inhibited, and thus, intermediates become prone to processing as a sort of "adaptation" to chronic replication stress. In contrast, the rapid activation of the "MUS81-dependent branch" of the replication fork recovery response, observed in the absence of WRN, would represent a "pathological" pathway adopted by WS cells because of the collapse of stalled forks (Fig. 7 D). This behavior resembles what is described in yeasts bearing mutations in the DNA polymerase α or δ (Murray et al., 1997; Kai et al., 2005). It is worthwhile to note that very recently, a recombination-independent function of MUS81 has been demonstrated in *S. pombe* yeast cells bearing mutations in replication checkpoint factors that resulted in replisome destabilization and fork collapse (Froget et al., 2008). Similarly, a recombination-independent function of MUS81 in response to replication arrest has been demonstrated in human cells (Shimura et al., 2008).

Two characteristic cellular phenotypes of WS cells are delayed S phase and asymmetrical elongation of DNA replication forks (Takeuchi et al., 1982; Rodriguez-Lopez et al., 2002). Our observations might contribute to give a mechanistic explanation for these phenotypes. Indeed, recombination engaged at collapsed forks would result in additional time to complete genome duplication as well as in an accumulation of gross chromosomal rearrangements (Myung et al., 2001), another characteristic feature of WS cells (Scappaticci et al., 1982; Grigorova et al., 2000).

In conclusion, our results demonstrate a novel role of WRN in preventing DSB induction and fork collapse after replication arrest, and contribute to support a function of WRN as a primary factor in the physiological response to stalled replication. Furthermore, our work uncovers the alternative pathway that is essential for the recovery of stalled replication forks in WS cells. Unscheduled generation of DSBs by MUS81 in WRN-deficient cells would grant cell viability, perhaps at the expense of genomic instability, contributing to the characteristic features of this genetic condition.

Materials and methods

Cell cultures

The SV40-transformed wild-type (MRC5SV) and WS fibroblasts (AG11395; Coriell Cell Repositories) were handled as described previously (Pichierri et al., 2004). The phenotypically reverted Epstein-Barr virus–transformed WS lymphoblastoid cell line (WS + WRN) and the parental lymphoblasts (AG14426) have been described previously (Franchitto et al., 2003).

Treatments and RNAi

To evaluate the effect of DNA replication arrest, wild-type and WS cells were treated with 2 mM HU for different times or with different doses of HU for 6 h. As otherwise indicated, etoposide was used at 50 μM for 6 h, a condition that has been found to cause an almost complete disassembly of the replisome (Montecucco et al., 2001).

ATR, MUS81, RAD51, or WRN expression was knocked down by transfection with a pool of four siRNAs directed against the coding sequence of the genes (SmartPool; Thermo Fisher Scientific). Transfection was performed using the HiPerfect reagent (QIAGEN) and 10 nM siRNA pool according to the manufacturer's instructions for adherent cells. Actual down-regulation was confirmed by Western blotting. As a control, an siRNA duplex directed against GFP was used (Pichierri et al., 2004). For the sake of clarity, data from the mock siRNA control were not included in figures. All the RNAi experiments were performed after 48 h from transfection and within ~72 h after transfection, when maximal inhibition of the expression of the target was observed.

PFGE

DNA fragmentation was analyzed only at different time points after treatment. High molecular weight genomic DNA was prepared in agarose blocks from exactly 10^6 cells as described previously (Lomonosov et al., 2003) and run on an 0.8% agarose/0.5% Tris/Borate/EDTA gel for 48 h on a Gene Navigator apparatus (GE Healthcare) at 70 V with a 20–30 min field switch time. DNA fragments from x 0.2 to 1 Mb appeared as a broadened compression band using our PFGE conditions.

Resolved DNA was stained with Sybr green (Invitrogen), and fragmented DNA quantitated from images was acquired using a GelDoc system (Alpha Innotech) and processed with ImageJ software (National Institutes of Health) after color inversion and contrast adjustment. DNA breakage was shown as arbitrary units after being normalized against total DNA contents. Values are given as a comparison against the level of DNA breakage of the matched untreated control. Representative images from triplicate experiments are shown.

Immunofluorescence

Immunofluorescence microscopy was performed on cells grown on coverslips. Except for RAD51 immunostaining, which was performed as described

previously (Pichierri et al., 2001), cells were fixed in 2% PFA/PBS for 20 min and permeabilized using 0.25% Triton X-100 for 10 min before being incubated with 5% normal serum/PBS for 60 min. After blocking, coverslips were incubated for 2 h with rabbit polyclonal anti–γ-H2AX antibody (1:1,000; Millipore) alone or in combination with either Alexa 488–conjugated anti-BrdU (1:500; Invitrogen) or sheep polyclonal anti–CENP-F (1:1,000; gift of S. Taylor, University of Manchester, Manchester, England, UK). Coverslips were then washed extensively, incubated with fluorescent secondary antibodies before being counterstained with DAPI, and observed with a 60× oil-immersion objective using an epifluorescence microscope (Leica) equipped with a charge-coupled device camera (Photometrics). Images were acquired as grayscale files using Metaview software (MDS Analytical Technologies) and processed using Photoshop (Adobe) to adjust contrast and brightness of the image. For each time point, at least 200 nuclei were examined, and foci were scored at a 60× magnification. Only nuclei showing more than five bright foci were considered to be positive. Parallel samples incubated with either the appropriate normal serum or only with the secondary antibody confirmed that the observed fluorescence pattern was not attributable to artifacts.

Western blot and chromatin fractionation

10^6 cells were trypsinized and collected by low-speed centrifugation, washed in PBS, and lysed in 300 µl of 2× electrophoresis sample buffer. One tenth of the lysate was loaded on 4–12% NuPage/MOPS gels (Invitrogen). Alternatively, proteins were separated on standard 6% or 8% SDS-PAGE. Blots were incubated separately (overnight at 4°C) with primary antibodies against MUS81 (1:2,000; AbCam), WRN (1:300; Santa Cruz Biotechnology, Inc.), β-tubulin (1:20,000; Sigma-Aldrich), pS345CHK1 (1:1,000; Cell Signaling Technology), PCNA (1:2,000; Santa Cruz Biotechnology, Inc.), CHK1, RAD52 (1:500; Santa Cruz Biotechnology, Inc.), and RAD51 (1:1,000; EMD). Horseradish peroxidase–conjugated goat species-specific secondary antibodies (Santa Cruz Biotechnology, Inc.) were used at a dilution of 1:2,000, and visualization of the signal was accomplished using Super Signal West Dura substrate (Thermo Fisher Scientific).

For the analysis of the PCNA, MUS81, RAD52, and RAD51 distribution in the chromatin fraction, 3×10^6 cells were processed as described previously (Pichierri et al., 2004). Chromatin-bound proteins were analyzed by Western blotting. Western blotting using an anti-H3 histone antibody (1:2,000; Millipore) or anti-ORC2 antibody (1:1,000; Santa Cruz Biotechnology, Inc.) served as a loading control for the chromatin fractions.

Quantification was performed on scanned images of blots using ImageJ software, and values shown on the graphs represent a percentage compared with the matched untreated control normalized against the protein content evaluated through histone H3 or ORC2 immunoblotting.

Flow cytometry analysis of PCNA association with chromatin

To analyze PCNA release from chromatin after treatments, cells were handled and analyzed by flow cytometry, as described previously (Scovassi and Prosperi, 2006). The amount of chromatin-associated PCNA was determined from the mean fluorescent intensity of the S-phase cells after gating as described in Fig. 2.

Evaluation of cellular viability and chromosomal damage

The sensitivity of cells to increasing doses of HU was evaluated by clonogenic survival. 24 h after transfection with the indicated siRNAs, SV40-transformed fibroblasts or HeLa cells were plated onto 60-mm dishes and cultured for an additional 24 h before exposure to HU for 14 h. After treatment, cells were grown for additional 7 d and fixed, then colony numbers were counted. Survival was expressed as a percentage of the number of clones in the untreated cultures, and values represent means ± SE from triplicate experiments. The analysis of the spontaneous and induced SCEs was performed on metaphase cells after treatment with 2 mM HU for 12 h, as described previously (Pichierri et al., 2000, 2004). When RNAi-treated cells were used, treatments were performed 48 h after transfection with siRNAs. A minimum of 200 metaphase cells was scored for each experimental point by two independent investigators.

Statistical analysis

All the reported data were evaluated pairwise comparing WS and wild-type cells. Data, with the exception of PCNA release from chromatin and chromosomal damage, are presented as mean ± SE and were derived from at least three repeated experiments. Data from PCNA release from chromatin and chromosomal damage are representative of at least duplicate experiments giving consistent results, and were evaluated using the analysis of variance test or Student's *t* test.

Synchronization procedure

Cell synchronization was accomplished by a double thymidine block. HeLa cells were plated and transfected with siRNAs as described previously (Pichierri et al., 2004). 8 h after transfection, thymidine was added to a final concentration of 2 mM and cells were incubated for 12 h. Cells were then washed twice with PBS and incubated with regular medium for 14 h before a second incubation with 2 mM thymidine for 12 h. 2 h after release from the second block, cells were exposed to 2 mM HU. Cells were collected at the indicated times and then processed for cell cycle analysis.

Cell cycle analysis by flow cytometry

30 min before HU treatment, cultures were pulse-labeled and chased with 45 µM BrdU to analyze progression through the cell cycle of the S-phase population. Alternatively, cultures were treated with 2 mM HU for different time points and pulsed with 45 µM BrdU for 30 min immediately prior to harvesting. When indicated, wild-type and WS fibroblasts were transfected with siRNA pool directed against MUS81 48 h before being exposed to 2 mM HU or 50 µM etoposide for the indicated times.

Cells were processed for flow cytometry as follows: for each time point, 10^6 cells were collected, and after two washes in PBS, fixed in 50% cold methanol. Then, cells were exposed to acid denaturation (3 M HCl), neutralization (1 M sodium tetraborate), and blocking solution (10% normal goat serum/PBS). After that, samples were incubated in series with a primary anti-BrdU antibody (1:100 in blocking solution) and then with a secondary FITC-conjugated antibody (1:50 in blocking solution). Samples were resuspended in 20 µg/ml propidium iodide before analysis.

Evaluation of DNA synthesis

For the evaluation of DNA synthesis, cells were exposed to 2 mM HU for 18 h, washed extensively, and recovered in drug-free medium for different time points. 45 µM BrdU was added 30 min before harvesting, and BrdU incorporation was analyzed as above. At least 500 interphase cells were scored to evaluate the percentage of labeled nuclei. Only nuclei displaying a distinct replicative pattern of BrdU labeling were considered to be actively replicating. The percentage of cells undergoing DNA synthesis at each time point was calculated as a fraction of the treated cells versus untreated controls.

For double BrdU/γ-H2AX immunostaining, cells were labeled with 45 µM BrdU for 30 min before being treated with 2 mM HU for 6 h. γ-H2AX immunofluorescence was performed as described previously (Pichierri et al., 2001), whereas BrdU detection was done after a postfixation step with a 3:1 methanol/acetic acid solution.

Evaluation of mitotic Index by phospho-H3 immunostaining

For evaluation of mitotic index, 3×10^5 cells were plated in 35-mm dishes and exposed to 2 mM HU for 3, 6, and 8 h before fixation in 2% PFA. After permeabilization in 0.5% Triton X-100, cells were blocked in 10% FBS and incubated with a 1:1,000 dilution of a polyclonal anti-pH3 rabbit antibody (Santa Cruz Biotechnology, Inc.) for 1 h at RT, followed by three washes in PBS and incubation with an Alexa 488–conjugated secondary antibody before DAPI counterstaining and evaluation of mitotic index by fluorescence microscopy.

DNA fiber assay

We measured the efficiency of replication recovery using the DNA fiber assay. First, DNA replication sites were labeled with 25 µM IdU (30 min), then cells were treated with 2 mM HU for 6 or 14 h to induce replication fork stalling. After treatment, cells were washed twice with PBS and incubated for 60 min in fresh medium with 100 µM CldU. To visualize sites of DNA replication, we prepared chromosomal DNA fibers on glass slides as described previously (Seiler et al., 2007). DNA fibers were analyzed through an epifluorescence microscope (Leica) equipped with a charge-coupled device camera. Images were acquired as grayscale files using Metaview software and then processed using Photoshop. Tracks containing IdU were pseudo-colored in red and represent all sites of DNA replication that were active before stalling. Tracks containing CldU were pseudo-colored in green and represent sites where DNA synthesis is recovered after HU removal. When CldU incorporation took place at previously stalled forks that remain active during the HU block, green tracks will start at sites of stalling with a certain degree of colocalization because of the limitation of the technique.

Significance of the difference between the means from the indicated genotypes was determined by a Student's *t* test.

Online supplemental material

Fig. S1 shows formation of DSBs in WS lymphoblasts. Fig. S2 shows that MUS81 down-regulation does not interfere with the inhibition of DNA

synthesis and cell cycle arrest after HU treatment. Fig. S3 shows cytofluorometric bivariate analysis of the HU-induced cell cycle perturbation. Fig. S4 shows analysis of replication fork restart after treatment with HU. Fig. S5 shows analysis of PCNA chromatin association after down-regulation of ATR by RNAi. Online supplemental material is available at http://www.jcb.org/cgi/content/full/jcb.200803173/DC1.

We would like to thank Dr. Chiara Conti (National Cancer Institute, National Institutes of Health, Bethesda, MD) for her assistance in setting up the DNA fiber assays and Dr. Stephen Taylor (University of Manchester, Manchester, England, UK) for providing the anti–CENP-F antiserum. We would like to thank Dr. Marco Crescenzi for the helpful discussion and critical reading of the manuscript.

This work was supported by individual grants from Telethon (grant GGP04094), Associazione Italiana per la Ricerca sul Cancro (AIRC), and Association for International Cancer Research (AICR, grant 07-0479) to P. Pichierri.

Submitted: 31 March 2008
Accepted: 19 September 2008

References

Arnaudeau, C., C. Lundin, and T. Helleday. 2001. DNA double-strand breaks associated with replication forks are predominantly repaired by homologous recombination involving an exchange mechanism in mammalian cells. *J. Mol. Biol.* 307:1235–1245.

Blais, V., H. Gao, C.A. Elwell, M.N. Boddy, P.H. Gaillard, P. Russell, and C.H. McGowan. 2004. RNA interference inhibition of Mus81 reduces mitotic recombination in human cells. *Mol. Biol. Cell.* 15:552–562.

Boddy, M.N., A. Lopez-Girona, P. Shanahan, H. Interthal, W.D. Heyer, and P. Russell. 2000. Damage tolerance protein Mus81 associates with the FHA1 domain of checkpoint kinase Cds1. *Mol. Cell. Biol.* 20:8758–8766.

Boddy, M.N., P.H. Gaillard, W.H. McDonald, P. Shanahan, J.R. Yates III, and P. Russell. 2001. Mus81-Eme1 are essential components of a Holliday junction resolvase. *Cell.* 107:537–548.

Branzei, D., and M. Foiani. 2005. The DNA damage response during DNA replication. *Curr. Opin. Cell Biol.* 17:568–575.

Casper, A.M., P. Nghiem, M.F. Arlt, and T.W. Glover. 2002. ATR regulates fragile site stability. *Cell.* 111:779–789.

Chen, L., and J. Oshima. 2002. Werner syndrome. *J. Biomed. Biotechnol.* 2:46–54.

Ciccia, A., A. Constantinou, and S.C. West. 2003. Identification and characterization of the human mus81-eme1 endonuclease. *J. Biol. Chem.* 278:25172–25178.

Cliby, W.A., C.J. Roberts, K.A. Cimprich, C.M. Stringer, J.R. Lamb, S.L. Schreiber, and S.H. Friend. 1998. Overexpression of a kinase-inactive ATR protein causes sensitivity to DNA-damaging agents and defects in cell cycle checkpoints. *EMBO J.* 17:159–169.

Cobb, J.A., L. Bjergbaek, K. Shimada, C. Frei, and S.M. Gasser. 2003. DNA polymerase stabilization at stalled replication forks requires Mec1 and the RecQ helicase Sgs1. *EMBO J.* 22:4325–4336.

Cotta-Ramusino, C., D. Fachinetti, C. Lucca, Y. Doksani, M. Lopes, J. Sogo, and M. Foiani. 2005. Exo1 processes stalled replication forks and counteracts fork reversal in checkpoint-defective cells. *Mol. Cell.* 17:153–159.

Dendouga, N., H. Gao, D. Moechars, M. Janicot, J. Vialard, and C.H. McGowan. 2005. Disruption of murine Mus81 increases genomic instability and DNA damage sensitivity but does not promote tumorigenesis. *Mol. Cell. Biol.* 25:7569–7579.

Doe, C.L., J.S. Ahn, J. Dixon, and M.C. Whitby. 2002. Mus81-Eme1 and Rqh1 involvement in processing stalled and collapsed replication forks. *J. Biol. Chem.* 277:32753–32759.

Fabre, F., A. Chan, W.D. Heyer, and S. Gangloff. 2002. Alternate pathways involving Sgs1/Top3, Mus81/ Mms4, and Srs2 prevent formation of toxic recombination intermediates from single-stranded gaps created by DNA replication. *Proc. Natl. Acad. Sci. USA.* 99:16887–16892.

Franchitto, A., and P. Pichierri. 2002. Protecting genomic integrity during DNA replication: correlation between Werner's and Bloom's syndrome gene products and the MRE11 complex. *Hum. Mol. Genet.* 11:2447–2453.

Franchitto, A., J. Oshima, and P. Pichierri. 2003. The G2-phase decatenation checkpoint is defective in Werner syndrome cells. *Cancer Res.* 63:3289–3295.

Fricke, W.M., S.A. Bastin-Shanower, and S.J. Brill. 2005. Substrate specificity of the *Saccharomyces cerevisiae* Mus81-Mms4 endonuclease. *DNA Repair (Amst.).* 4:243–251.

Froget, B., J. Blaisonneau, S. Lambert, and G. Baldacci. 2008. Cleavage of stalled forks by fission yeast mus81/eme1 in absence of DNA replication checkpoint. *Mol. Biol. Cell.* 19:445–456.

Gao, H., X.B. Chen, and C.H. McGowan. 2003. Mus81 endonuclease localizes to nucleoli and to regions of DNA damage in human S-phase cells. *Mol. Biol. Cell.* 14:4826–4834.

Grigorova, M., A.S. Balajee, and A.T. Natarajan. 2000. Spontaneous and X-ray-induced chromosomal aberrations in Werner syndrome cells detected by FISH using chromosome-specific painting probes. *Mutagenesis.* 15:303–310.

Haber, J.E., and W.D. Heyer. 2001. The fuss about Mus81. *Cell.* 107:551–554.

Hanada, K., M. Budzowska, M. Modesti, A. Maas, C. Wyman, J. Essers, and R. Kanaar. 2006. The structure-specific endonuclease Mus81-Eme1 promotes conversion of interstrand DNA crosslinks into double-strands breaks. *EMBO J.* 25:4921–4932.

Hanada, K., M. Budzowska, S.L. Davies, E. van Drunen, H. Onizawa, H.B. Beverloo, A. Maas, J. Essers, I.D. Hickson, and R. Kanaar. 2007. The structure-specific endonuclease Mus81 contributes to replication restart by generating double-strand DNA breaks. *Nat. Struct. Mol. Biol.* 14:1096–1104.

Hickson, I.D. 2003. RecQ helicases: caretakers of the genome. *Nat. Rev. Cancer.* 3:169–178.

Interthal, H., and W.D. Heyer. 2000. MUS81 encodes a novel helix-hairpin-helix protein involved in the response to UV- and methylation-induced DNA damage in *Saccharomyces cerevisiae*. *Mol. Gen. Genet.* 263:812–827.

Ira, G., A. Malkova, G. Liberi, M. Foiani, and J.E. Haber. 2003. Srs2 and Sgs1-Top3 suppress crossovers during double-strand break repair in yeast. *Cell.* 115:401–411.

Kai, M., M.N. Boddy, P. Russell, and T.S. Wang. 2005. Replication checkpoint kinase Cds1 regulates Mus81 to preserve genome integrity during replication stress. *Genes Dev.* 19:919–932.

Kaliraman, V., J.R. Mullen, W.M. Fricke, S.A. Bastin-Shanower, and S.J. Brill. 2001. Functional overlap between Sgs1-Top3 and the Mms4-Mus81 endonuclease. *Genes Dev.* 15:2730–2740.

Khakhar, R.R., J.A. Cobb, L. Bjergbaek, I.D. Hickson, and S.M. Gasser. 2003. RecQ helicases: multiple roles in genome maintenance. *Trends Cell Biol.* 13:493–501.

Lambert, S., and B.S. Lopez. 2001. Role of RAD51 in sister-chromatid exchanges in mammalian cells. *Oncogene.* 20:6627–6631.

Lomonosov, M., S. Anand, M. Sangrithi, R. Davies, and A.R. Venkitaraman. 2003. Stabilization of stalled DNA replication forks by the BRCA2 breast cancer susceptibility protein. *Genes Dev.* 17:3017–3022.

Lucca, C., F. Vanoli, C. Cotta-Ramusino, A. Pellicioli, G. Liberi, J. Haber, and M. Foiani. 2004. Checkpoint-mediated control of replisome-fork association and signalling in response to replication pausing. *Oncogene.* 23:1206–1213.

McPherson, J.P., B. Lemmers, R. Chahwan, A. Pamidi, E. Migon, E. Matysiak-Zablocki, M.E. Moynahan, J. Essers, K. Hanada, A. Poonepalli, et al. 2004. Involvement of mammalian Mus81 in genome integrity and tumor suppression. *Science.* 304:1822–1826.

Merrick, C.J., D. Jackson, and J.F. Diffley. 2004. Visualization of altered replication dynamics after DNA damage in human cells. *J. Biol. Chem.* 279:20067–20075.

Montecucco, A., R. Rossi, G. Ferrari, A.I. Scovassi, E. Prosperi, and G. Biamonti. 2001. Etoposide induces the dispersal of DNA ligase I from replication factories. *Mol. Biol. Cell.* 12:2109–2118.

Mullen, J.R., V. Kaliraman, S.S. Ibrahim, and S.J. Brill. 2001. Requirement for three novel protein complexes in the absence of the Sgs1 DNA helicase in *Saccharomyces cerevisiae*. *Genetics.* 157:103–118.

Murray, J.M., H.D. Lindsay, C.A. Munday, and A.M. Carr. 1997. Role of *Schizosaccharomyces pombe* RecQ homolog, recombination, and checkpoint genes in UV damage tolerance. *Mol. Cell. Biol.* 17:6868–6875.

Myung, K., A. Datta, and R.D. Kolodner. 2001. Suppression of spontaneous chromosomal rearrangements by S phase checkpoint functions in *Saccharomyces cerevisiae*. *Cell.* 104:397–408.

Osman, F., and M.C. Whitby. 2007. Exploring the roles of Mus81-Eme1/Mms4 at perturbed replication forks. *DNA Repair (Amst.).* 6:1004–1017.

Pichierri, P., A. Franchitto, P. Mosesso, L. Proietti de Santis, A.S. Balajee, and F. Palitti. 2000. Werner's syndrome lymphoblastoid cells are hypersensitive to topoisomerase II inhibitors in the G2 phase of the cell cycle. *Mutat. Res.* 459:123–133.

Pichierri, P., A. Franchitto, P. Mosesso, and F. Palitti. 2001. Werner's syndrome protein is required for correct recovery after replication arrest and DNA damage induced in S-phase of cell cycle. *Mol. Biol. Cell.* 12:2412–2421.

Pichierri, P., A. Franchitto, and F. Rosselli. 2004. BLM and the FANC proteins collaborate in a common pathway in response to stalled replication forks. *EMBO J.* 23:3154–3163.

Rattner, J.B., A. Rao, M.J. Fritzler, D.W. Valencia, and T.J. Yen. 1993. CENP-F is a .ca 400 kDa kinetochore protein that exhibits a cell-cycle dependent localization. *Cell Motil. Cytoskeleton.* 26:214–226.

Rodriguez-Lopez, A.M., D.A. Jackson, F. Iborra, and L.S. Cox. 2002. Asymmetry of DNA replication fork progression in Werner's syndrome. *Aging Cell.* 1:30–39.

Rossi, R., M.R. Lidonnici, S. Soza, G. Biamonti, and A. Montecucco. 2006. The dispersal of replication proteins after etoposide treatment requires the cooperation of Nbs1 with the ataxia telangiectasia Rad3-related/Chk1 pathway. *Cancer Res.* 66:1675–1683.

Saintigny, Y., F. Delacote, G. Vares, F. Petitot, S. Lambert, D. Averbeck, and B.S. Lopez. 2001. Characterization of homologous recombination induced by replication inhibition in mammalian cells. *EMBO J.* 20:3861–3870.

Saintigny, Y., K. Makienko, C. Swanson, M.J. Emond, and R.J. Monnat Jr. 2002. Homologous recombination resolution defect in werner syndrome. *Mol. Cell. Biol.* 22:6971–6978.

Scappaticci, S., D. Cerimele, and M. Fraccaro. 1982. Clonal structural chromosomal rearrangements in primary fibroblast cultures and in lymphocytes of patients with Werner's syndrome. *Hum. Genet.* 62:16–24.

Scovassi, A.I., and E. Prosperi. 2006. Analysis of proliferating cell nuclear antigen (PCNA) associated with DNA excision repair sites in mammalian cells. *Methods Mol. Biol.* 314:457–475.

Seiler, J.A., C. Conti, A. Syed, M.I. Aladjem, and Y. Pommier. 2007. The intra-S-phase checkpoint affects both DNA replication initiation and elongation: single-cell and -DNA fiber analyses. *Mol. Cell. Biol.* 27:5806–5818.

Shimura, T., M.J. Torres, M.M. Martin, V.A. Rao, Y. Pommier, M. Katsura, K. Miyagawa, and M.I. Aladjem. 2008. Bloom's syndrome helicase and Mus81 are required to induce transient double-strand DNA breaks in response to DNA replication stress. *J. Mol. Biol.* 375:1152–1164.

Takeuchi, F., F. Hanaoka, M. Goto, M. Yamada, and T. Miyamoto. 1982. Prolongation of S phase and whole cell cycle in Werner's syndrome fibroblasts. *Exp. Gerontol.* 17:473–480.

Taylor, A.M. 2001. Chromosome instability syndromes. *Best Pract. Res. Clin. Haematol.* 14:631–644.

Trenz, K., E. Smith, S. Smith, and V. Costanzo. 2006. ATM and ATR promote Mre11 dependent restart of collapsed replication forks and prevent accumulation of DNA breaks. *EMBO J.* 25:1764–1774.

Ward, I.M., and J. Chen. 2001. Histone H2AX is phosphorylated in an ATR-dependent manner in response to replicational stress. *J. Biol. Chem.* 276:47759–47762.

Whitby, M.C., F. Osman, and J. Dixon. 2003. Cleavage of model replication forks by fission yeast Mus81-Eme1 and budding yeast Mus81-Mms4. *J. Biol. Chem.* 278:6928–6935.

Wu, L., and I.D. Hickson. 2003. The Bloom's syndrome helicase suppresses crossing over during homologous recombination. *Nature.* 426:870–874.

Yamagata, K., J. Kato, A. Shimamoto, M. Goto, Y. Furuichi, and H. Ikeda. 1998. Bloom's and Werner's syndrome genes suppress hyperrecombination in yeast sgs1 mutant: implication for genomic instability in human diseases. *Proc. Natl. Acad. Sci. USA*. 95:8733–8738.